Interfaces and Free Boundaries **11** (2009), 515–536

Second order numerical scheme for motion of polygonal curves with constant area speed

MICHAL BENEŠ
Department of Mathematics, Faculty of Nuclear Sciences and Physical Engineering, Czech Technical University in Prague, Trojanova 13, 120 00 Praha, Czech Republic
E-mail: michal.benes@fjfi.cvut.cz

MASATO KIMURA
Faculty of Mathematics, Kyushu University, 6-10-1 Hakozaki, Fukuoka 812-8581, Japan
E-mail: masato@math.kyushu-u.ac.jp

SHIGETOSHI YAZAKI
Faculty of Engineering, University of Miyazaki, 1-1 Gakuen Kibanadai Nishi, Miyazaki 889-2192, Japan
E-mail: yazaki@cc.miyazaki-u.ac.jp

[Received 25 July 2008 and in revised form 25 March 2009]

We study polygonal analogues of several moving boundary problems and their time discretization which preserves the constant area speed property. We establish various polygonal analogues of geometric formulas for moving boundaries and make use of the geometric formulas for our numerical scheme to analyse general constant area speed motion of polygons. Accuracy and efficiency of our numerical scheme are checked through numerical simulations for several polygonal motions such as motion by curvature and area-preserving advected flow etc.

2010 Mathematics Subject Classification: 35R35, 39A12, 53C44, 65L20.

Keywords: motion of polygons; moving boundary problem; crystalline motion; crystalline curvature; motion by curvature; constant area speed motion; area-preserving numerical scheme; second order scheme.

1. Introduction

In this article, we focus on polygonal motion given by moving boundary problems, which is restricted to an equivalence class of polygons. We introduce a notion of polygonal curvature, which is consistent with polygonal analogues of geometric variational formulae.

We propose a formulation of general area-preserving motion of polygonal curves by using a system of ODEs. The moving polygon belongs to a prescribed class of polygons, which is similar to the admissible class in the theory of crystalline motion by curvature. There are many articles about the crystalline curvature flow and asymptotic behavior of solutions. To select just a few, we refer to the pioneering work [2], [11], and to [1, 5, 6, 8, 9, 10, 14, 15, 16, 17]. In particular, if the initial curve is a convex polygon in a crystalline admissible class, then our polygonal curvature flow is nothing but the crystalline curvature flow. However, we consider more general polygonal moving boundary problems in wider admissible classes of polygons. For example, we can consider polygons shown in Figures 4 and 5 in our equivalence classes, but they are not admissible in the sense of the crystalline curvature flow.

Based on the formulation of general polygonal moving boundary problems, we propose an implicit time discretization scheme with an effective iteration scheme for the nonlinear system at each time step. It has second order accuracy and preserves the constant area speed property. In a fixed admissible class of polygons, we prove a second order convergence theorem for our numerical scheme.

On the other hand, it is expected that our polygonal analogue becomes a natural approximate solution of a smooth moving boundary problem if the number of edges is large enough. It would be an important and interesting application of our polygonal motion, which is not considered in this paper. We only mention here that the crystalline algorithm and the corresponding convergence theorems for the motion by curvature can be found in [5, 6, 7, 8, 11, 12, 13].

The organization of this paper is as follows. Fundamental notation and formulas for polygons and polygonal motions are introduced in Section 2. In Section 3, a general initial value problem for polygonal motion in an equivalence class is considered, and the constant area speed condition is introduced. Several basic examples of polygonal motions such as the polygonal curvature flow and the polygonal advected flow are also presented. In Section 4, an implicit scheme of Crank–Nicolson type and an iteration scheme for the nonlinear system at each time step are proposed. The proposed scheme inherits the constant area speed property and its second order convergence is proved in Theorem 4.5. In Section 5, the accuracy of our numerical scheme is checked through various numerical simulations in comparison with the first order explicit Euler scheme. These simulations show that the second order scheme preserves the constant area speed property with high accuracy.

2. Polygons and polygonal motions

We give basic definitions and notation for the polygonal motion in an equivalence class of polygons, In particular, polygonal curvature is introduced as a generalization of crystalline curvature. We also provide fundamental formulae and properties in this section.

2.1 *Polygons*

We define a set of polygons in $\mathbb{R}^2$ by

$$\mathcal{P} := \{\Gamma;\ \Gamma \text{ is a polygonal Jordan curve in } \mathbb{R}^2\}.$$

In this paper, we assume that any two-dimensional vector $\boldsymbol{x} \in \mathbb{R}^2$ is represented by a column vector, and we denote its transposed row vector by $\boldsymbol{x}^{\mathrm{T}}$. For $\Gamma \in \mathcal{P}$, the bounded interior polygonal domain surrounded by Γ is denoted by Ω. For simplicity, we assume that Ω is simply connected, but many of the following arguments are valid in other geometrical situations.

Let $\Gamma \in \mathcal{P}$ be an N-polygon. The N vertices of Γ are denoted by $\boldsymbol{w}_j \in \mathbb{R}^2$ for $j = 1, \ldots, N$ counterclockwise, where $\boldsymbol{w}_0 = \boldsymbol{w}_N$ and $\boldsymbol{w}_{N+1} = \boldsymbol{w}_1$. Hereafter we use the periodic numbering convention $\mathsf{F}_0 = \mathsf{F}_N$ and $\mathsf{F}_{N+1} = \mathsf{F}_1$ for any quantities defined for N-polygons.

For $j = 1, \ldots, N$, the jth edge between $\boldsymbol{w}_{j-1}$ and $\boldsymbol{w}_j$ is defined by

$$\Gamma_j = \{(1-\theta)\boldsymbol{w}_{j-1} + \theta \boldsymbol{w}_j;\ 0 < \theta < 1\},$$

and its length is denoted by $|\Gamma_j| := |\boldsymbol{w}_j - \boldsymbol{w}_{j-1}|$. The characteristic function $\chi_j \in L^\infty(\Gamma)$ for Γ_j is defined as

$$\chi_j(\boldsymbol{x}) := \begin{cases} 1, & \boldsymbol{x} \in \Gamma_j \\ 0, & \boldsymbol{x} \in \Gamma \setminus \Gamma_j \end{cases} \qquad (j = 1, \ldots, N).$$

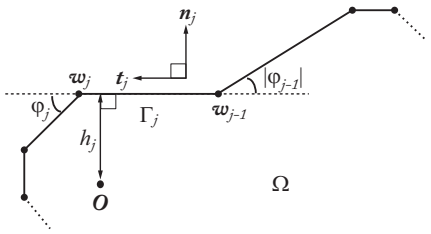

FIG. 1. Some quantities defined on Γ_j.

The outward unit normal on Γ_j is denoted by $\boldsymbol{n}_j$, and the outer angle at the vertex $\boldsymbol{w}_j$ is denoted by $\varphi_j \in (-\pi, \pi) \setminus \{0\}$. They satisfy $\cos\varphi_j = \boldsymbol{n}_{j+1} \cdot \boldsymbol{n}_j$. We also define the height of Γ_j with respect to the origin by $h_j := \boldsymbol{w}_j \cdot \boldsymbol{n}_j = \boldsymbol{w}_{j-1} \cdot \boldsymbol{n}_j$ (see Figure 1).

Then the straight line including Γ_j is expressed by the equation $\boldsymbol{n}_j \cdot \boldsymbol{x} = h_j$, and the vertices of $\Gamma \in \mathcal{P}$ are given from $\{h_j\}_j$ as

$$\boldsymbol{w}_j = \begin{pmatrix} \boldsymbol{n}_j^{\mathrm{T}} \\ \boldsymbol{n}_{j+1}^{\mathrm{T}} \end{pmatrix}^{-1} \begin{pmatrix} h_j \\ h_{j+1} \end{pmatrix} \quad (j = 1, \ldots, N). \tag{2.1}$$

PROPOSITION 2.1 Under the above conditions, we have

$$|\Gamma_j| = a_{j-1}h_{j-1} + b_j h_j + a_j h_{j+1} \quad (j = 1, \ldots, N), \tag{2.2}$$

where $a_j := \operatorname{cosec}\varphi_j$ and $b_j := -\cot\varphi_{j-1} - \cot\varphi_j$.

Proof. We define a unit tangent vector of Γ_j by $\boldsymbol{t}_j := (\boldsymbol{w}_j - \boldsymbol{w}_{j-1})/|\Gamma_j|$. We remark that $\boldsymbol{n}_{j+1} \cdot \boldsymbol{t}_j = -\boldsymbol{n}_j \cdot \boldsymbol{t}_{j+1} = \sin\varphi_j$ and $\boldsymbol{t}_j \cdot \boldsymbol{t}_{j+1} = \cos\varphi_j$. Then, from (2.1) and the equality

$$\begin{pmatrix} \boldsymbol{n}_j^{\mathrm{T}} \\ \boldsymbol{n}_{j+1}^{\mathrm{T}} \end{pmatrix} (-\boldsymbol{t}_{j+1} \quad \boldsymbol{t}_j) = \begin{pmatrix} -\boldsymbol{n}_j \cdot \boldsymbol{t}_{j+1} & 0 \\ 0 & \boldsymbol{n}_{j+1} \cdot \boldsymbol{t}_j \end{pmatrix} = \frac{1}{a_j} \begin{pmatrix} 1 & 0 \\ 0 & 1 \end{pmatrix},$$

we have

$$\boldsymbol{w}_j = a_j \begin{pmatrix} -\boldsymbol{t}_{j+1} & \boldsymbol{t}_j \end{pmatrix} \begin{pmatrix} h_j \\ h_{j+1} \end{pmatrix} = -\boldsymbol{t}_{j+1} a_j h_j + \boldsymbol{t}_j a_j h_{j+1}.$$

Since

$$\begin{aligned} |\Gamma_j| = \boldsymbol{t}_j \cdot (\boldsymbol{w}_j - \boldsymbol{w}_{j-1}) &= \boldsymbol{t}_j \cdot \{(-\boldsymbol{t}_{j+1} a_j h_j + \boldsymbol{t}_j a_j h_{j+1}) - (-\boldsymbol{t}_j a_{j-1} h_{j-1} + \boldsymbol{t}_{j-1} a_{j-1} h_j)\} \\ &= a_j h_{j+1} - \{a_j \cos\varphi_j + a_{j-1}\cos\varphi_{j-1}\} h_j + a_{j-1} h_{j-1} = a_j h_{j+1} + b_j h_j + a_{j-1} h_{j-1}, \end{aligned}$$

we obtain the formula (2.2). □

The total length of Γ is given by

$$|\Gamma| := \sum_{j=1}^{N} |\Gamma_j| = \sum_{j=1}^{N} (a_j + b_j + a_{j-1}) h_j = \sum_{j=1}^{N} \eta_j h_j, \tag{2.3}$$

where $\eta_j := a_j + b_j + a_{j-1} = \tan(\varphi_j/2) + \tan(\varphi_{j-1}/2)$. The area of the interior domain Ω is denoted by $|\Omega|$, which is given by

$$|\Omega| = \frac{1}{2}\sum_{j=1}^{N} |\Gamma_j| h_j. \tag{2.4}$$

The above symbols are also written as $\boldsymbol{n}_j = \boldsymbol{n}_j(\Gamma)$, $a_j = a_j(\Gamma)$, $h_j = h_j(\Gamma)$ etc., whenever we need to distinguish them from quantities for other polygons.

2.2 *Equivalence classes of polygons*

We define an equivalence relation for polygons $\Gamma, \Sigma \in \mathcal{P}$. We say that Γ is equivalent to Σ ($\Gamma \sim \Sigma$) if their numbers of edges are the same (say N) and $\boldsymbol{n}_j(\Gamma) = \boldsymbol{n}_j(\Sigma)$ for all $j = 1, \ldots, N$ after choosing suitable counterclockwise numbering for Γ and Σ. The equivalence class of $\Gamma \in \mathcal{P}$ is denoted by $\mathcal{P}[\Gamma] := \{\Sigma \in \mathcal{P};\ \Sigma \sim \Gamma\}$.

We fix an N-polygon $\Gamma^* \in \mathcal{P}$ and set $\mathcal{P}^* := \mathcal{P}[\Gamma^*]$. We define the distance between Γ and Σ in $\mathcal{P}^*$ by

$$d(\Gamma, \Sigma) := \max_{j=1,\ldots,N} |h_j(\Gamma) - h_j(\Sigma)|.$$

It is clear that $(\mathcal{P}^*, d)$ is a metric space, since it is isometrically embedded in $\mathbb{R}^N$ equipped with the maximum norm $|\cdot|_\infty$ by the height function $\boldsymbol{h}$ defined by

$$\boldsymbol{h}(\Gamma) := (h_1(\Gamma), \ldots, h_N(\Gamma)) \in \mathbb{R}^N \quad (\Gamma \in \mathcal{P}^*).$$

We assume that vectors in $\mathbb{R}^N$ are represented by row vectors. It is obvious that the image $\boldsymbol{h}(\mathcal{P}^*)$ of the height function is open in $\mathbb{R}^N$.

For $\Gamma \in \mathcal{P}^*$ and $\varepsilon > 0$, an ε-ball in $\mathcal{P}^* = \mathcal{P}[\Gamma]$ with center Γ is denoted by

$$B(\Gamma, \varepsilon) := \{\Sigma \in \mathcal{P}[\Gamma];\ d(\Sigma, \Gamma) < \varepsilon\}.$$

For an open set $\mathcal{O} \subset \mathcal{P}^*$ and $\Gamma \in \mathcal{O}$, we define a number $\rho(\Gamma, \mathcal{O}) > 0$ as

$$\rho(\Gamma, \mathcal{O}) := \inf\{|\boldsymbol{a} - \boldsymbol{h}(\Gamma)|_\infty;\ \boldsymbol{a} \in \mathbb{R}^N \setminus \boldsymbol{h}(\mathcal{O})\}.$$

We remark that $\rho(\cdot, \mathcal{O})$ is Lipschitz continuous with Lipschitz constant 1:

$$|\rho(\Gamma, \mathcal{O}) - \rho(\Sigma, \mathcal{O})| \leqslant d(\Gamma, \Sigma) \quad (\Gamma, \Sigma \in \mathcal{O}).$$

For a compact set $\mathcal{K} \subset \mathcal{O}$, we also define

$$\rho(\mathcal{K}, \mathcal{O}) := \min_{\Gamma \in \mathcal{K}} \rho(\Gamma, \mathcal{O}).$$

Let $a_j = a_j(\Gamma^*)$ and $b_j = b_j(\Gamma^*)$. Then from (2.2), we obtain

$$\begin{aligned} \big||\Gamma_j| - |\Sigma_j|\big| &= |a_{j-1}(h_{j-1}(\Gamma) - h_{j-1}(\Sigma)) + b_j(h_j(\Gamma) - h_j(\Sigma)) + a_j(h_{j+1}(\Gamma) - h_{j+1}(\Sigma))| \\ &\leqslant C^* d(\Gamma, \Sigma) \quad (j = 1, \ldots, N), \end{aligned}$$

where we define

$$C^* := \max_{l=1,\dots,N} \{|a_{l-1}| + |b_l| + |a_l|\}. \tag{2.5}$$

For any $\Gamma^0, \Gamma^1 \in \mathcal{P}^*$ and for $\theta \in [0, 1]$, we define

$$\boldsymbol{h}^\theta := (1-\theta)\boldsymbol{h}(\Gamma^0) + \theta \boldsymbol{h}(\Gamma^1) \in \mathbb{R}^N.$$

If there exists $\Gamma^\theta \in \mathcal{P}^*$ with $\boldsymbol{h}(\Gamma^\theta) = \boldsymbol{h}^\theta$, then Γ^θ is called the θ-*interpolation* of Γ^0 and Γ^1, and denoted by $(1-\theta)\Gamma^0 + \theta\Gamma^1 := \Gamma^\theta \in \mathcal{P}^*$.

2.3 *Polygonal motions*

We consider a moving polygon $\Gamma(t) \in \mathcal{P}$, where the parameter t (time) belongs to an interval $\mathcal{I} \subset \mathbb{R}$. For $k \in \mathbb{N} \cup \{0\}$, we say that a moving polygon $\Gamma(t)$ is of class C^k on $\mathcal{I}$ if the number of edges of $\Gamma(t)$ does not change in time and $\boldsymbol{w}_j \in C^k(\mathcal{I};\ \mathbb{R}^2)$ for all $j = 1, \dots, N$.

If $k \geqslant 1$, we can define the normal velocity at $\boldsymbol{x} \in \Gamma_j(t)$, the jth edge of $\Gamma(t)$. Let $\boldsymbol{n}_j(t) := \boldsymbol{n}_j(\Gamma(t))$. We suppose $\boldsymbol{x}^* \in \Gamma_j(t^*)$ and $\boldsymbol{x}^* = (1-\theta)\boldsymbol{w}_{j-1}(t^*) + \theta \boldsymbol{w}_j(t^*)$ for some $\theta \in (0, 1)$, and define $\boldsymbol{x}(\theta, t) := (1-\theta)\boldsymbol{w}_{j-1}(t) + \theta \boldsymbol{w}_j(t) \in \Gamma_j(t)$. Then the *outward normal velocity* of $\Gamma_j(t^*)$ at $\boldsymbol{x}^*$ is defined by

$$V_j(\boldsymbol{x}^*, t^*) := \dot{\boldsymbol{x}}(\theta, t^*) \cdot \boldsymbol{n}_j(t^*) = (1-\theta)\dot{\boldsymbol{w}}_{j-1}(t^*) \cdot \boldsymbol{n}_j(t^*) + \theta \dot{\boldsymbol{w}}_j(t^*) \cdot \boldsymbol{n}_j(t^*).$$

Hereafter, the (partial) derivative of F with respect to t is denoted by $\dot{\mathsf{F}}$. We remark that $V_j(\cdot, t)$ is linear function along each $\Gamma_j(t)$. We define the *normal velocity* of $\Gamma(t)$ by

$$V(\cdot, t) := \sum_{j=1}^{N} V_j(\cdot, t)\chi_j(\cdot, t) \in L^\infty(\Gamma(t)),$$

where $\chi_j(\cdot, t) \in L^\infty(\Gamma(t))$ is the characteristic function of $\Gamma_j(t)$.

If a moving polygon $\Gamma(t)$ belongs to a fixed equivalence class $\mathcal{P}^*$ for all $t \in \mathcal{I}$, it is called a *polygonal motion in* $\mathcal{P}^*$ in this paper. Let $\boldsymbol{h}(t) = (h_1(t), \dots, h_N(t)) \in \mathbb{R}^N$ be the height function for $\Gamma(t)$. We remark that a polygonal motion $\Gamma(t)$ in $\mathcal{P}^*$ ($t \in \mathcal{I}$) is of class C^k if and only if $\boldsymbol{h} \in C^k(\mathcal{I};\ \mathbb{R}^N)$, from (2.1). If $\Gamma(t)$ is a C^1 polygonal motion in $\mathcal{P}^*$, its normal velocity V_j of $\Gamma_j(t)$ is constant on each $\Gamma_j(t)$ and it is given by $V_j(t) = \dot{h}_j(t)$. We denote by $\Omega(t)$ the interior domain surrounded by $\Gamma(t)$.

PROPOSITION 2.2 Let $\Gamma(t)$ be a C^1 polygonal motion in $\mathcal{P}^*$. Then

$$\frac{\mathrm{d}}{\mathrm{d}t}|\Omega(t)| = \int_{\Gamma(t)} V(\boldsymbol{x}, t)\,\mathrm{d}s = \sum_{j=1}^{N} |\Gamma_j(t)| V_j(t). \tag{2.6}$$

Proof. From (2.2) and (2.4), we obtain

$$\begin{aligned}\frac{\mathrm{d}}{\mathrm{d}t}|\Omega(t)| &= \frac{\mathrm{d}}{\mathrm{d}t}\left(\frac{1}{2}\sum_{j=1}^{N} |\Gamma_j(t)| h_j(t)\right) = \frac{1}{2}\sum_{j=1}^{N} (\{a_{j-1}V_{j-1} + b_j V_j + a_j V_{j+1}\}h_j + |\Gamma_j| V_j) \\ &= \frac{1}{2}\sum_{j=1}^{N} V_j\{a_j h_{j+1} + b_j h_j + a_{j-1}h_{j-1}\} + \frac{1}{2}\sum_{j=1}^{N} |\Gamma_j| V_j = \sum_{j=1}^{N} |\Gamma_j| V_j. \qquad \square\end{aligned}$$

For $\Gamma \in \mathcal{P}^*$, the *polygonal curvature* κ_j of Γ_j is defined by

$$\kappa_j := \frac{\eta_j}{|\Gamma_j|}, \qquad \eta_j := \tan\frac{\varphi_j}{2} + \tan\frac{\varphi_{j-1}}{2}.$$

We also define the polygonal curvature of Γ by

$$\kappa := \sum_{j=1}^{N} \kappa_j \chi_j \in L^\infty(\Gamma).$$

The reason why this is called "curvature" is shown by the following proposition.

PROPOSITION 2.3 Let $\Gamma(t)$ $(t \in \mathcal{I})$ be a C^1 polygonal motion in $\mathcal{P}^*$. Then

$$\frac{\mathrm{d}}{\mathrm{d}t}|\Gamma(t)| = \sum_{j=1}^{N} |\Gamma_j(t)|\kappa_j(t)V_j(t) = \int_{\Gamma(t)} \kappa(\boldsymbol{x}, t)V(\boldsymbol{x}, t)\, ds.$$

Proof. We obtain

$$\frac{\mathrm{d}}{\mathrm{d}t}|\Gamma(t)| = \frac{\mathrm{d}}{\mathrm{d}t}\sum_{j=1}^{N} \eta_j h_j(t) = \sum_{j=1}^{N} \eta_j V_j(t) = \sum_{j=1}^{N} |\Gamma_j(t)|\kappa_j(t)V_j(t),$$

from the formula (2.3). □

When the initial curve is a convex polygon, or a non-convex but admissible polygon, the polygonal curvature coincides with the crystalline curvature in the crystalline motion theory ([2, 11]). We, however, consider wider polygon classes and more general moving boundary problems. For example, we can construct a non-convex polygon whose edges all have a constant positive polygonal curvature $\kappa_1 = \cdots = \kappa_N > 0$ (see Section 5.2.4). Such polygons are excluded in the standard crystalline theory.

3. Initial value problem of polygonal motion

We consider initial value problems of polygonal motions in an equivalence class. A general polygonal motion problem is formulated as a system of ODEs with respect to the height function. The notion of constant area speed (CAS, for short) is introduced and a necessary and sufficient condition for it is given. Several concrete examples of polygonal motion problems with the CAS property are also presented.

3.1 *General polygonal motion problem*

We fix an equivalence class $\mathcal{P}^*$ of N-polygons as in Section 2.3. For an open set $\mathcal{O} \subset \mathcal{P}^*$ and $T_* \in (0, \infty]$, let $\boldsymbol{F} = (F_1, \ldots, F_N)$ be a given continuous function from $\mathcal{O} \times [0, T_*)$ to $\mathbb{R}^N$ with the local Lipschitz property: For every compact set $\mathcal{K} \subset \mathcal{O}$ and $T \in (0, T_*)$, there exists $L(\mathcal{K}, T) > 0$ such that

$$|\boldsymbol{F}(\Gamma, t) - \boldsymbol{F}(\Sigma, t)|_\infty \leqslant L(\mathcal{K}, T)d(\Gamma, \Sigma) \quad (\Gamma, \Sigma \in \mathcal{K},\ t \in [0, T]). \tag{3.1}$$

Under the condition (3.1), for a compact set $\mathcal{K} \subset \mathcal{O}$ and $T \in (0, T_*)$, we also define

$$M(\mathcal{K}, T) := \max\{|\boldsymbol{F}(\Gamma, t)|_\infty;\ \Gamma \in \mathcal{K},\ t \in [0, T]\} > 0.$$

We consider the following initial value problem of polygonal motion.

PROBLEM 3.1 For a given N-polygon $\Gamma^* \in \mathcal{O}$, find a C^1 polygonal motion $\Gamma(t) \in \mathcal{O}$ $(0 \leqslant t \leqslant T < T_*)$ such that

$$\begin{cases} V_j(t) = F_j(\Gamma(t), t) \quad (t \in [0, T],\ j = 1, \dots, N), \\ \Gamma(0) = \Gamma^*. \end{cases}$$

Under the Lipschitz condition (3.1), it is clear that there exists a local solution $\Gamma(t)$ in a short time interval $[0, T]$, since Problem 3.1 can be expressed as an initial value problem for ordinary differential equations for $\boldsymbol{h}(t)$.

We consider the following assumption on F_j:

$$\sum_{j=1}^{N} |\Gamma_j| F_j(\Gamma, t) = \mu_{\mathrm{CAS}} \quad (\Gamma \in \mathcal{O},\ t \in [0, T_*)), \tag{3.2}$$

where μ_{CAS} is a fixed real number. Under the assumption (3.2), from the formula (2.6), any solution $\Gamma(t)$ to Problem 3.1 has the following property of *constant area speed* (CAS):

$$\frac{\mathrm{d}}{\mathrm{d}t}|\Omega(t)| = \mu_{\mathrm{CAS}}.$$

3.2 *Examples of polygonal motion problems*

In this section, we give some examples of polygonal motions. For several moving boundary problems for smooth curves, we can construct their polygonal analogues which naturally satisfy the basic properties such as CAS and curve shortening (CS, for short).

PROBLEM 3.2 (polygonal curvature flow) For a given N-polygon $\Gamma^* \in \mathcal{P}^*$, find a C^1 family of N-polygons $\bigcup_{0 \leqslant t \leqslant T} \Gamma(t) \subset \mathcal{P}^*$ $(T < T_*)$ satisfying

$$\begin{cases} V_j(t) = -\kappa_j(t) \quad (t \in [0, T],\ j = 1, \dots, N), \\ \Gamma(0) = \Gamma^*. \end{cases}$$

This is a polygonal analogue of the curvature flow (curve shortening problem, see [4] and references therein). In the theory of crystalline motion, Problem 3.2 is considered in a crystalline admissible class and is called the crystalline curvature motion.

Similar to the curvature flow for smooth curves, the solution of Problem 3.2 has the CS property:

$$\frac{\mathrm{d}}{\mathrm{d}t}|\Gamma(t)| = \sum_{j=1}^{N} |\Gamma_j(t)| \kappa_j(t) V_j(t) = -\sum_{j=1}^{N} |\Gamma_j(t)| \kappa_j(t)^2 \leqslant 0,$$

and the CAS property with $\mu_{\mathrm{CAS}} = -2\sum_{j=1}^{N} \tan(\varphi_j/2)$:

$$\frac{\mathrm{d}}{\mathrm{d}t}|\Omega(t)| = -\sum_{j=1}^{N} |\Gamma_j(t)| \kappa_j(t) = -\sum_{j=1}^{N} \eta_j = -2\sum_{j=1}^{N} \tan\frac{\varphi_j}{2} = \text{const.}$$

A numerical example will be shown in Figure 2 (left).

PROBLEM 3.3 (area-preserving polygonal curvature flow) For a given N-polygon $\Gamma^* \in \mathcal{P}^*$, find a C^1 family of N-polygons $\bigcup_{0\leqslant t\leqslant T} \Gamma(t) \subset \mathcal{P}^*$ $(T < T_*)$ satisfying

$$\begin{cases} V_j(t) = \langle \kappa(\cdot,t)\rangle - \kappa_j(t) & (t \in [0,T],\ j = 1,\dots,N), \\ \Gamma(0) = \Gamma^*. \end{cases}$$

Here $\langle \kappa(\cdot,t)\rangle$ is the mean value of κ on $\Gamma(t)$:

$$\langle \kappa(\cdot,t)\rangle = \frac{1}{|\Gamma(t)|}\int_{\Gamma(t)} \kappa(\boldsymbol{x},t)\,\mathrm{d}s = \frac{\sum_{i=1}^N \eta_i}{|\Gamma(t)|} = \frac{2\sum_{i=1}^N \tan(\varphi_i/2)}{|\Gamma(t)|}.$$

This is a polygonal analogue of the area-preserving curvature flow (see e.g. [3]). Similar to the area-preserving curvature flow for smooth curves, the solution of Problem 3.3 has the CS property:

$$\frac{\mathrm{d}}{\mathrm{d}t}|\Gamma(t)| = \sum_{j=1}^N |\Gamma_j(t)|\kappa_j(t)V_j(t) = -\sum_{j=1}^N |\Gamma_j(t)|(\kappa_j(t) - \langle\kappa(\cdot,t)\rangle)^2 \leqslant 0,$$

and the CAS property with $\mu_{\mathrm{CAS}} = 0$:

$$\frac{\mathrm{d}}{\mathrm{d}t}|\Omega(t)| = \langle\kappa(\cdot,t)\rangle|\Gamma(t)| - \int_{\Gamma(t)} \kappa(\boldsymbol{x},t)\,\mathrm{d}s = 0.$$

Some numerical examples will be shown in Figure 4.

In what follows, the mean value of F on the edge Γ_j is denoted by

$$\langle \mathsf{F}\rangle_j := \frac{1}{|\Gamma_j|}\int_{\Gamma_j} \mathsf{F}(\boldsymbol{x})\,\mathrm{d}s.$$

Let G be a bounded Lipschitz domain in $\mathbb{R}^2$. We define

$$\mathcal{O}_G := \{\Gamma \in \mathcal{P}^*;\ \Omega(\Gamma) \supset \overline{G}\}.$$

PROBLEM 3.4 (polygonal advected flow with constant area speed) Let $\boldsymbol{u} \in C^1(\mathbb{R}^2 \setminus G;\ \mathbb{R}^2)$ with $\operatorname{div}\boldsymbol{u} = 0$ in $\mathbb{R}^2 \setminus \overline{G}$. For a given N-polygon $\Gamma^* \in \mathcal{O}_G$, find a C^1 family of N-polygons $\bigcup_{0\leqslant t\leqslant T} \Gamma(t) \subset \mathcal{O}_G$ $(T < T_*)$ satisfying

$$\begin{cases} V_j(t) = \langle \boldsymbol{u}\rangle_j \cdot \boldsymbol{n}_j & (t \in [0,T],\ j = 1,\dots,N), \\ \Gamma(0) = \Gamma^*. \end{cases}$$

The solution has the CAS property with $\mu_{\mathrm{CAS}} = \int_{\partial G} \boldsymbol{n}\cdot\boldsymbol{u}\,\mathrm{d}s$:

$$\begin{aligned} \frac{\mathrm{d}}{\mathrm{d}t}|\Omega(t)| &= \sum_{j=1}^N |\Gamma_j(t)|\,\langle\boldsymbol{u}\rangle_j \cdot \boldsymbol{n}_j = \sum_{j=1}^N \int_{\Gamma_j(t)} \boldsymbol{u}\cdot\boldsymbol{n}_j\,\mathrm{d}s \\ &= \int_{\partial G} \boldsymbol{u}\cdot\boldsymbol{n}\,\mathrm{d}s - \int_{\Omega(t)\setminus\overline{G}} \operatorname{div}\boldsymbol{u}\,\mathrm{d}\boldsymbol{x} = \int_{\partial G} \boldsymbol{u}\cdot\boldsymbol{n}\,\mathrm{d}s, \end{aligned}$$

where $\boldsymbol{n}$ is the unit normal vector on ∂G pointing to the interior of G. A numerical example will be shown in Figure 6.

4. Numerical schemes

We propose an implicit time discretization of Crank–Nicolson type to solve the general initial value problem of polygonal motions (Problem 3.1) and show that it preserves the CAS property and has a second order accuracy. We also propose an effective iteration scheme to solve a nonlinear system which appears at each time step. For comparison, we also consider an explicit Euler scheme. We additionally give comments on the curve shortening and constant length speed properties and their numerical preservation.

4.1 *Notation*

In Section 4, we consider time discretization of Problem 3.1 with the following notation. The discrete time steps are denoted by $0 = t_0 < t_1 < \cdots < t_{\bar{m}} \leqslant T$. The step size, which may be nonuniform, and the maximum size are defined by

$$\tau_m := t_{m+1} - t_m \quad (m = 0, 1, \ldots, \bar{m} - 1), \qquad \tau := \max_{0 \leqslant m < \bar{m}} \tau_m.$$

An approximate solution of $\Gamma(t_m)$ is denoted by $\Gamma^m \in \mathcal{P}^*$. Quantities pertaining to the polygon Γ^m are denoted by $\boldsymbol{h}^m = (h_1^m, \ldots, h_N^m) := (h_1(\Gamma^m), \ldots, h_N(\Gamma^m), \kappa_j^m := \kappa_j(\Gamma^m)$, etc. We define $\boldsymbol{e}^m := \boldsymbol{h}(t_m) - \boldsymbol{h}^m \in \mathbb{R}^N$. Then we have $d(\Gamma(t_m), \Gamma^m) = |\boldsymbol{e}^m|_\infty$.

The discrete normal velocity $\boldsymbol{V}^m = (V_1^m, \ldots, V_N^m)$, which is an approximation of $\boldsymbol{V}(t_m) = \dot{\boldsymbol{h}}(t_m)$, is defined by

$$\boldsymbol{V}^m := \frac{\boldsymbol{h}^{m+1} - \boldsymbol{h}^m}{\tau_m} \quad (m = 0, 1, \ldots, \bar{m} - 1). \tag{4.1}$$

Corresponding to the formula (2.6), we have

$$\frac{|\Omega^{m+1}| - |\Omega^m|}{\tau_m} = \sum_{j=1}^{N} \frac{|\Gamma_j^m| + |\Gamma_j^{m+1}|}{2} V_j^m. \tag{4.2}$$

This has the form of the sum of the areas of N trapezoids and is derived from (2.4) as follows:

$$\begin{aligned} |\Omega^{m+1}| - |\Omega^m| &= \frac{1}{2} \sum_{j=1}^{N} (|\Gamma_j^{m+1}| h_j^{m+1} - |\Gamma_j^m| h_j^m) \\ &= \frac{1}{2} \sum_{j=1}^{N} \{(|\Gamma_j^{m+1}| + |\Gamma_j^m|)(h_j^{m+1} - h_j^m) + |\Gamma_j^{m+1}| h_j^m - |\Gamma_j^m| h_j^{m+1}\} \\ &= \frac{\tau_m}{2} \sum_{j=1}^{N} (|\Gamma_j^{m+1}| + |\Gamma_j^m|) V_j^m + \frac{1}{2} \sum_{j=1}^{N} (|\Gamma_j^{m+1}| h_j^m - |\Gamma_j^m| h_j^{m+1}), \end{aligned}$$

where the last sum is equal to zero due to the equality (2.2).

In the following sections, we suppose that there exists a unique solution $\Gamma(t)$ for $0 \leqslant t \leqslant T < T_*$ to Problem 3.1 under the condition (3.1), and that discrete time steps $0 = t_0 < t_1 < \cdots < t_{\bar{m}} \leqslant T$ are given a priori with uniform time step, so $t_m = m\tau$. We adopt the uniform time increment in the numerical examples in Section 5. It is, however, possible to apply any a posteriori adaptive time step

control scheme. Similar to the finite time extinction of the curvature flow of smooth curves, even in polygonal motions, the solution polygon often has singularities in finite time. For instance, $|\Gamma_j(t)|$ tends to zero, in other words, $|\kappa_j(t)|$ tends to infinity. A posteriori adaptive time step control will be required near the blow-up time for accurate computation.

4.2 *Second order implicit scheme*

We consider the following implicit scheme for Problem 3.1.

PROBLEM 4.1 For a given N-polygon $\Gamma_* \in \mathcal{O}$ and given time steps $0 = t_0 < t_1 < \cdots < t_{\bar{m}} \leqslant T$, find polygons $\Gamma^m \in \mathcal{O}$ $(m = 1, \ldots, \bar{m})$ such that

$$\begin{cases} V_j^m = F_j(\Gamma^{m+1/2}, t_{m+1/2}) \quad (m = 0, 1, \ldots, \bar{m} - 1,\ j = 1, \ldots, N), \\ \Gamma^0 = \Gamma_*, \end{cases}$$

where $\Gamma^{m+1/2}$ and $t_{m+1/2}$ are the $1/2$-interpolations:

$$\Gamma^{m+1/2} := \frac{\Gamma^m + \Gamma^{m+1}}{2} \in \mathcal{P}^*, \qquad t_{m+1/2} := \frac{t_m + t_{m+1}}{2} = t_m + \frac{\tau_m}{2}.$$

This is a generalized version of the scheme presented in [13] for the area-preserving crystalline curvature flow.

PROPOSITION 4.2 Suppose the CAS property (3.2) holds. Let $\Gamma^m \in \mathcal{O}$ $(m = 1, \ldots, \bar{m})$ be a solution of Problem 4.1. Then

$$|\Omega^{m+1}| = |\Omega^m| + \mu_{\mathrm{CAS}}\tau_m \qquad (m = 0, 1, \ldots, \bar{m} - 1).$$

In other words, $|\Omega^m| = |\Omega(t_m)|$ if the exact solution $\Omega(t)$ of Problem 3.1 exists.

Proof. Since $|\Gamma_j^{m+1/2}| = (|\Gamma_j^m| + |\Gamma_j^{m+1}|)/2$, we have

$$\frac{|\Omega^{m+1}| - |\Omega^m|}{\tau_m} = \sum_{j=1}^{N} |\Gamma_j^{m+1/2}| F_j(\Gamma^{m+1/2}, t_{m+1/2}) = \mu_{\mathrm{CAS}},$$

from formula (4.2). □

We remark that the numerical scheme of Problem 4.1 inherits the CAS property but does not depend on the area speed μ_{CAS}.

Since Problem 4.1 is an implicit scheme, it is not clear whether $\Gamma^{m+1} \in \mathcal{O}$ can be determined uniquely from the previous polygon $\Gamma^m \in \mathcal{O}$, the time t_m, and the time step size τ_m. Another question is how to solve the equations

$$\boldsymbol{h}^{m+1} = \boldsymbol{h}^m + \tau_m \boldsymbol{F}\left(\frac{\Gamma^m + \Gamma^{m+1}}{2}, t_{m+1/2}\right) \tag{4.3}$$

to obtain (an approximation of) Γ^{m+1} numerically. Answers to these questions will be given in Theorems 4.4 and 4.5.

We fix $\hat{\Gamma} \in \mathcal{O}$ and $\hat{t} \in [0, T)$, which correspond to Γ^m and $t_{m+1/2}$, respectively. Let $\mathcal{K}$ be a compact convex set in $\mathcal{P}^*$ with $\hat{\Gamma} \in \mathcal{K} \subset \mathcal{O}$. For $\Sigma \in \mathcal{K}$ and $\hat{\tau} \in (0, \rho(\hat{\Gamma}, \mathcal{O})M(\mathcal{K}, T)^{-1})$, we can define $\tilde{\Sigma} \in \mathcal{O}$ by

$$\boldsymbol{h}(\tilde{\Sigma}) = \boldsymbol{h}(\hat{\Gamma}) + \hat{\tau}\boldsymbol{F}\left(\frac{\hat{\Gamma} + \Sigma}{2}, \hat{t}\right).$$

We define $\Lambda(\Sigma) := \Lambda(\Sigma; \hat{\Gamma}, \hat{t}, \hat{\tau}) =: \tilde{\Sigma}$. Then Λ becomes a mapping from $\mathcal{K}$ to $\mathcal{O}$. We have the following lemma.

LEMMA 4.3 Let $\varepsilon \in (0, \rho(\hat{\Gamma}, \mathcal{O}))$ and $\lambda \in (0, 1)$ be fixed, and let $\hat{\mathcal{K}} := \overline{B(\hat{\Gamma}, \varepsilon)}$. Suppose that

$$0 < \hat{\tau} \leqslant \min\left\{T - \hat{t}, \frac{\varepsilon}{M(\hat{\mathcal{K}}, T)}, \frac{2\lambda}{L(\hat{\mathcal{K}}, T)}\right\}.$$

Then Λ maps $\hat{\mathcal{K}}$ into $\hat{\mathcal{K}}$ and satisfies

$$d(\Lambda(\Sigma^1), \Lambda(\Sigma^2)) \leqslant \lambda d(\Sigma^1, \Sigma^2) \quad (\Sigma^1, \Sigma^2 \in \hat{\mathcal{K}}). \tag{4.4}$$

Hence Λ is a contraction mapping on $\hat{\mathcal{K}}$ and there exists a unique fixed point of Λ in $\hat{\mathcal{K}}$.

Proof. Let $\Sigma \in \hat{\mathcal{K}}$. Since $\hat{\mathcal{K}}$ is convex, it follows that $(\hat{\Gamma} + \Sigma)/2 \in \hat{\mathcal{K}}$. We also have

$$|\boldsymbol{h}(\tilde{\Sigma}) - \boldsymbol{h}(\hat{\Gamma})|_\infty = \left|\hat{\tau}\boldsymbol{F}\left(\frac{\hat{\Gamma} + \Sigma}{2}, \hat{t}\right)\right|_\infty \leqslant \hat{\tau} M(\hat{\mathcal{K}}, T) \leqslant \varepsilon.$$

This estimate shows that Λ is a mapping from $\hat{\mathcal{K}}$ into itself. The estimate (4.4) is proved as follows:

$$\begin{aligned} d(\Lambda(\Sigma^1), \Lambda(\Sigma^2)) &= |\boldsymbol{h}(\Lambda(\Sigma^1)) - \boldsymbol{h}(\Lambda(\Sigma^2))|_\infty = \hat{\tau}\left|\boldsymbol{F}\left(\frac{\hat{\Gamma} + \Sigma^1}{2}, \hat{t}\right) - \boldsymbol{F}\left(\frac{\hat{\Gamma} + \Sigma^2}{2}, \hat{t}\right)\right|_\infty \\ &\leqslant \hat{\tau} L(\hat{\mathcal{K}}, T) d\left(\frac{\hat{\Gamma} + \Sigma^1}{2}, \frac{\hat{\Gamma} + \Sigma^2}{2}\right) \\ &= \hat{\tau} L(\hat{\mathcal{K}}, T)\left|\frac{\boldsymbol{h}(\hat{\Gamma}) + \boldsymbol{h}(\Sigma^1)}{2} - \frac{\boldsymbol{h}(\hat{\Gamma}) + \boldsymbol{h}(\Sigma^2)}{2}\right|_\infty \\ &= \frac{\hat{\tau}}{2} L(\hat{\mathcal{K}}, T) d(\Sigma^1, \Sigma^2) \leqslant \lambda d(\Sigma^1, \Sigma^2). \end{aligned}$$

□

The following theorem gives us an efficient numerical scheme to obtain Γ^{m+1}. The proof is clear from Lemma 4.3.

THEOREM 4.4 Let $\mathcal{K}$ be a compact set in $\mathcal{O}$ and let $\varepsilon \in (0, \rho(\mathcal{K}, \mathcal{O}))$. Define

$$\mathcal{K}_\varepsilon := \overline{\bigcup_{\Sigma \in \mathcal{K}} B(\Sigma, \varepsilon)}.$$

For fixed m $(< \bar{m})$ in Problem 4.1, assume that $\Gamma^m \in \mathcal{K}$ and

$$\tau_m \leqslant \min\left\{\frac{\varepsilon}{M(\mathcal{K}_\varepsilon, T)}, \frac{2\lambda}{L(\mathcal{K}_\varepsilon, T)}\right\},$$

where $\lambda \in (0, 1)$. Then there exists a unique $\Gamma^{m+1} \in \overline{B(\Gamma^m, \varepsilon)}$ satisfying (4.3).

Furthermore, Γ^{m+1} is a fixed point of the contraction $\Lambda_m := \Lambda(\cdot\,; \Gamma^m, t_m, \tau_m)$ in $\overline{B(\Gamma^m, \varepsilon)}$, and is given by the limit of $\Lambda_m^\nu(\Gamma^m)$ as $\nu \to \infty$ with the following estimate:

$$d(\Gamma^{m+1}, \Lambda_m^\nu(\Gamma^m)) \leqslant \lambda^\nu d(\Gamma^{m+1}, \Gamma^m) \quad (\nu \in \mathbb{N}).$$

From this theorem, $\Lambda_m^\nu(\Gamma^m)$ for ν sufficiently large gives a satisfactory approximation of Γ^{m+1}. An iteration algorithm based on this idea will be given in Section 5.1. The following theorem shows the second order convergence of the implicit numerical scheme of Problem 4.1.

THEOREM 4.5 Suppose that $\{\Gamma(t)\}_{0\leqslant t\leqslant T}$ is a C^{k+1} solution of Problem 3.1 for $k = 0$, 1, or 2. There exist $\delta^* > 0$, $\tau^* > 0$, $C > 0$ and a non-decreasing function $\omega(a) > 0$ with

$$\omega(a) = \begin{cases} o(a^k) & \text{if } k = 0 \text{ or } 1, \\ O(a^2) & \text{if } k = 2, \end{cases} \qquad \text{as } a \downarrow 0, \tag{4.5}$$

such that if $d(\Gamma^*, \Gamma^0) \leqslant \delta^*$ and $\tau \leqslant \tau^*$, then $\Gamma^m \in \mathcal{O}$ $(m = 1, \ldots, \bar{m})$ are inductively determined by the implicit scheme of Problem 4.1, and

$$\max_{0\leqslant m\leqslant \bar{m}} d(\Gamma(t_m), \Gamma^m) \leqslant \omega(\tau) + Cd(\Gamma(0), \Gamma^0).$$

Proof. We put $\hat{\rho} := \rho(\{\Gamma(t);\ 0 \leqslant t \leqslant T\}, \mathcal{O})$, and fix $\delta \in (0, \hat{\rho})$ and $\varepsilon \in (0, \hat{\rho} - \delta)$. We define

$$\begin{aligned} &\mathcal{K} := \overline{\bigcup_{0\leqslant t\leqslant T} B(\Gamma(t), \delta)}, \qquad \mathcal{K}_\varepsilon := \overline{\bigcup_{\Sigma\in\mathcal{K}} B(\Sigma, \varepsilon)}, \\ &L := L(\mathcal{K}_\varepsilon, T), \qquad R(a) := e^{L/2}(1 - aL/2)^{-1/a} \quad (0 < a < 2/L), \\ &p_m := |e^m|_\infty + \omega(\tau)/L \quad (m = 0, 1, \ldots, \bar{m}), \end{aligned}$$

where a non-decreasing function $\omega(a)$ $(0 < a < T)$ which satisfies (4.5) will be defined later in (4.9). Since $R(\cdot)$ is an increasing function, there exist $\delta^* > 0$ and $\tau^* > 0$ such that

$$R(\tau^*)^T(\delta^* + \omega(\tau^*)/L) \leqslant \delta, \qquad \tau^* < \min(\varepsilon/M(\mathcal{K}_\varepsilon, T),\ 2/L).$$

For $m = 0, 1, \ldots, \bar{m} - 1$, we will prove the following inductive conditions:

$$\Gamma^m \in \mathcal{K},\ p_m \leqslant R(\tau)^{t_m} p_0 \ \Rightarrow\ \exists \Gamma^{m+1} \in \mathcal{K},\ p_{m+1} \leqslant R(\tau)^{t_{m+1}} p_0. \tag{4.6}$$

The conditions $\Gamma^0 \in \mathcal{K}$ and $p_0 \leqslant R(\tau)^0 p_0$ for the case $m = 0$ are obviously satisfied.

Assume that $\Gamma^m \in \mathcal{K}$ and $p_m \leqslant R(\tau)^{t_m} p_0$ for a fixed m. Then, from Theorem 4.4, there exists a unique Γ^{m+1} in $\overline{B(\Gamma^m, \varepsilon)} \subset \mathcal{K}_\varepsilon$, and we have

$$\boldsymbol{e}^{m+1} - \boldsymbol{e}^m = \boldsymbol{h}(t_{m+1}) - \boldsymbol{h}(t_m) - \tau_m \boldsymbol{V}^m = \tau_m\{\boldsymbol{\xi}^m + (\boldsymbol{V}(t_{m+1/2}) - \boldsymbol{V}^m)\}, \tag{4.7}$$

where

$$\boldsymbol{\xi}^m := \frac{\boldsymbol{h}(t_{m+1}) - \boldsymbol{h}(t_m)}{\tau_m} - \dot{\boldsymbol{h}}(t_{m+1/2}).$$

The last term of (4.7) is estimated as follows. Since $\Gamma(t_{m+1/2}) \in \mathcal{K} \subset \mathcal{K}_\varepsilon$ and $\Gamma^{m+1/2} \in \overline{B(\Gamma^m, \varepsilon)} \subset \mathcal{K}_\varepsilon$, we have

$$\begin{aligned} |\boldsymbol{V}(t_{m+1/2}) - \boldsymbol{V}^m|_\infty &= |\boldsymbol{F}(\Gamma(t_{m+1/2}), t_{m+1/2}) - \boldsymbol{F}(\Gamma^{m+1/2}, t_{m+1/2})|_\infty \\ &\leqslant Ld(\Gamma(t_{m+1/2}), \Gamma^{m+1/2}) = L\left|\boldsymbol{h}(t_{m+1/2}) - \frac{\boldsymbol{h}^m + \boldsymbol{h}^{m+1}}{2}\right|_\infty \\ &= L\left|\frac{1}{2}(\boldsymbol{e}^m + \boldsymbol{e}^{m+1}) - \boldsymbol{\zeta}^m\right|_\infty, \end{aligned} \tag{4.8}$$

where

$$\boldsymbol{\zeta}^m := \frac{\boldsymbol{h}(t_m) + \boldsymbol{h}(t_{m+1})}{2} - \boldsymbol{h}(t_{m+1/2}).$$

Combining (4.7) and (4.8), we obtain

$$\begin{aligned} |\boldsymbol{e}^{m+1}|_\infty &\leqslant |\boldsymbol{e}^m|_\infty + \tau_m\,|\boldsymbol{\xi}^m|_\infty + \tau_m L\left|\frac{1}{2}(\boldsymbol{e}^m + \boldsymbol{e}^{m+1}) - \boldsymbol{\zeta}^m\right|_\infty \\ &\leqslant |\boldsymbol{e}^m|_\infty + \frac{\tau_m L}{2}(|\boldsymbol{e}^{m+1}|_\infty + |\boldsymbol{e}^m|_\infty) + \tau_m(|\boldsymbol{\xi}^m|_\infty + L|\boldsymbol{\zeta}^m|_\infty). \end{aligned}$$

By the Taylor expansion, we can obtain a non-decreasing function $\omega(a)$ $(0 < a < T)$ which satisfies the condition (4.5) and the inequality

$$|\boldsymbol{\xi}^m|_\infty + L|\boldsymbol{\zeta}^m|_\infty \leqslant \omega(\tau). \tag{4.9}$$

Hence,

$$(1 - \tau_m L/2)|\boldsymbol{e}^{m+1}|_\infty \leqslant (1 + \tau_m L/2)|\boldsymbol{e}^m|_\infty + \tau_m \omega(\tau),$$

and this inequality is equivalent to

$$(1 - \tau_m L/2)\,p_{m+1} \leqslant (1 + \tau_m L/2)\,p_m.$$

From the inequalities

$$(1 - \tau_m L/2) \geqslant (1 - \tau L/2)^{\tau_m/\tau} \quad \text{and} \quad (1 + \tau_m L/2) \leqslant e^{\tau_m L/2},$$

we obtain

$$p_{m+1} \leqslant (1 - \tau_m L/2)^{-1}(1 + \tau_m L/2)\,p_m \leqslant R(\tau)^{\tau_m}(R(\tau)^{t_m} p_0) = R(\tau)^{t_{m+1}} p_0.$$

The condition $\Gamma^{m+1} \in \mathcal{K}$ follows from this estimate as

$$|\boldsymbol{e}^{m+1}|_\infty \leqslant p_{m+1} \leqslant R(\tau^*)^{t_{m+1}}\, p_0 \leqslant R(\tau^*)^T(\delta^* + \omega(\tau^*)/L) \leqslant \delta.$$

Hence, we have proved (4.6), which leads us to the estimate

$$|\boldsymbol{e}^m|_\infty \leqslant R(\tau^*)^T(|\boldsymbol{e}^0|_\infty + \omega(\tau)/L) - \omega(\tau)/L \leqslant R(\tau^*)^T|\boldsymbol{e}^0|_\infty + \frac{R(\tau^*)^T - 1}{L}\omega(\tau).$$

The assertion of the theorem is obtained by putting $C := R(\tau^*)^T$ and denoting the last term $L^{-1}(R(\tau^*)^T - 1)\omega(\tau)$ again by $\omega(\tau)$. □

4.3 *Euler scheme*

For Problem 3.1, one of the simplest numerical schemes is the following explicit Euler scheme:

PROBLEM 4.6 For a given N-polygon $\Gamma_* \in \mathcal{O}$ and time steps $0 = t_0 < t_1 < \cdots < t_{\bar{m}} \leqslant T$, find polygons $\Gamma^m \in \mathcal{O}$ $(m = 1, \ldots, \bar{m})$ such that

$$\begin{cases} V_j^m = F_j(\Gamma^m, t_m) \quad (m = 0, 1, \ldots, \bar{m} - 1,\ j = 1, \ldots, N), \\ \Gamma^0 = \Gamma_*. \end{cases}$$

The explicit Euler scheme is simple but it has only first order accuracy. In particular, for polygonal motions with the CAS property, we are required to use a more accurate scheme such as Problem 4.1 in order to keep its CAS property numerically. Similarly to the case of the implicit scheme (Theorem 4.5), the convergence theorem for the Euler scheme is stated as follows.

THEOREM 4.7 Suppose the condition (3.1) holds and $\{\Gamma(t)\}_{0 \leqslant t \leqslant T}$ is a C^{k+1} solution of Problem 3.1 for $k = 0$ or 1. There exist $\delta^* > 0$, $\tau^* > 0$, $C > 0$ and a non-decreasing function $\omega(a) > 0$ with

$$\omega(a) = \begin{cases} o(1) & \text{if } k = 0, \\ O(a) & \text{if } k = 1, \end{cases} \qquad \text{as } a \downarrow 0, \tag{4.10}$$

such that if $d(\Gamma^*, \Gamma^0) \leqslant \delta^*$ and $\tau \leqslant \tau^*$, then $\Gamma^m \in \mathcal{O}$ $(m = 1, \ldots, \bar{m})$ is determined by the Euler scheme of Problem 4.6 and satisfies the estimate

$$\max_{0 \leqslant m \leqslant \bar{m}} d(\Gamma(t_m), \Gamma^m) \leqslant \omega(\tau) + Cd(\Gamma(0), \Gamma^0).$$

Proof. We define

$$\boldsymbol{\xi}^m := \frac{\boldsymbol{h}(t_{m+1}) - \boldsymbol{h}(t_m)}{\tau_m} - \dot{\boldsymbol{h}}(t_m) \quad (m = 0, 1, \ldots, \bar{m} - 1).$$

Then, by the Taylor expansion, we are able to find a non-decreasing function $\omega(a)$ $(0 < a < T)$ which satisfies the condition (4.10) and the inequality

$$|\boldsymbol{\xi}^m|_\infty \leqslant \omega(\tau). \tag{4.11}$$

We put $\hat{\rho} := \rho(\{\Gamma(t);\ 0 \leqslant t \leqslant T\}, \mathcal{O})$, and fix $\delta \in (0, \hat{\rho})$ and $\varepsilon \in (0, \hat{\rho} - \delta)$. We define

$$\mathcal{K} := \overline{\bigcup_{0 \leqslant t \leqslant T} B(\Gamma(t), \delta)}, \qquad \mathcal{K}_\varepsilon := \overline{\bigcup_{\Sigma \in \mathcal{K}} B(\Sigma, \varepsilon)},$$
$$L := L(\mathcal{K}, T), \qquad p_m := |\boldsymbol{e}^m|_\infty + \omega(\tau)/L \quad (m = 0, 1, \ldots, \bar{m}).$$

There exist $\delta^* > 0$ and $\tau^* > 0$ such that

$$e^{TL}(\delta^* + \omega(\tau^*)/L) \leqslant \delta, \qquad \tau^* \leqslant \varepsilon / M(\mathcal{K}, T).$$

For $m = 0, 1, \ldots, \bar{m} - 1$, we will prove the following inductive conditions:

$$\Gamma^m \in \mathcal{K},\ p_m \leqslant e^{t_m L} p_0 \ \Rightarrow\ \exists \Gamma^{m+1} \in \mathcal{K},\ p_{m+1} \leqslant e^{t_{m+1} L} p_0. \tag{4.12}$$

The condition for $m = 0$ is obviously satisfied.

Assume that $\Gamma^m \in \mathcal{K}$ and $p_m \leqslant e^{t_m L} p_0$ for a fixed m. Then, from the condition $\tau^* \leqslant \varepsilon / M(\mathcal{K}, T)$, Γ^{m+1} belongs to $\overline{B(\Gamma^m, \varepsilon)} \subset \mathcal{K}_\varepsilon$, and we have

$$\boldsymbol{e}^{m+1} - \boldsymbol{e}^m = \boldsymbol{h}(t_{m+1}) - \boldsymbol{h}(t_m) - \tau_m \boldsymbol{V}^m = \tau_m \{\boldsymbol{\xi}^m + (\boldsymbol{V}(t_m) - \boldsymbol{V}^m)\}. \tag{4.13}$$

Since $\Gamma(t_m)$ and Γ^m both belong to $\mathcal{K}$, we have

$$|\boldsymbol{V}(t_m) - \boldsymbol{V}^m|_\infty = |\boldsymbol{F}(\Gamma(t_m), t_m) - \boldsymbol{F}(\Gamma^m, t_m)|_\infty \leqslant L d(\Gamma(t_m), \Gamma^m) = L|\boldsymbol{e}^m|_\infty. \tag{4.14}$$

Combining (4.11), (4.13) and (4.14), we obtain

$$|\boldsymbol{e}^{m+1}|_\infty \leqslant (1 + \tau_m L)|\boldsymbol{e}^m|_\infty + \tau_m \omega(\tau),$$

and

$$p_{m+1} \leqslant (1 + \tau_m L) p_m \leqslant e^{\tau_m L}(e^{t_m L} p_0) = e^{t_{m+1} L} p_0.$$

Since

$$|\boldsymbol{e}^{m+1}|_\infty \leqslant p_{m+1} \leqslant e^{t_{m+1} L} p_0 \leqslant e^{TL}(\delta^* + \omega(\tau^*)/L) \leqslant \delta,$$

the condition $\Gamma^{m+1} \in \mathcal{K}$ follows. Hence, we have proved (4.12), which leads us to the estimate

$$|\boldsymbol{e}^m|_\infty \leqslant e^{LT}(|\boldsymbol{e}^0|_\infty + \omega(\tau)/L) - \omega(\tau)/L \leqslant e^{LT}|\boldsymbol{e}^0|_\infty + \frac{e^{LT} - 1}{L}\omega(\tau).$$

The desired assertion is obtained by putting $C := e^{LT}$ and denoting the last term $L^{-1}(e^{LT} - 1)\omega(\tau)$ again by $\omega(\tau)$. □

4.4 *Curve shortening and constant length speed property*

As can be seen in Section 3.2, many moving boundary problems have the CS property:

$$\frac{\mathrm{d}}{\mathrm{d}t}|\Gamma(t)| \leqslant 0.$$

From (2.3), a necessary and sufficient condition for the CS property is

$$\sum_{j=1}^{N} \eta_j F_j(\Gamma, t) \leqslant 0 \quad (\Gamma \in \mathcal{O},\ t \in [0, T_*)). \tag{4.15}$$

Similarly to the CAS property (3.2), we can also consider the constant length speed (CLS, for short) property:

$$\frac{\mathrm{d}}{\mathrm{d}t}|\Gamma(t)| = \mu_{\mathrm{CLS}}.$$

A necessary and sufficient condition for the CLS property is

$$\sum_{j=1}^{N} \eta_j F_j(\Gamma, t) = \mu_{\mathrm{CLS}} \quad (\Gamma \in \mathcal{O},\ t \in [0, T_*)). \tag{4.16}$$

An example with the CLS property is the constant speed motion:

$$F_j(\Gamma, t) = 1 \quad (j = 1, \ldots, N), \qquad \mu_{\mathrm{CLS}} = 2 \sum_{j=1}^{N} \tan \frac{\varphi_j}{2}.$$

Another example is the length-preserving polygonal curvature flow:

$$F_j(\Gamma, t) = \frac{\sum_{i=1}^{N} |\Gamma_j|\, \kappa_j(\Gamma)^2}{2\sum_{i=1}^{N} \tan(\varphi_i/2)} - \kappa_j(\Gamma) \quad (j = 1, \ldots, N), \qquad \mu_{\mathrm{CLS}} = 0. \tag{4.17}$$

It is easy to check that both the second order implicit scheme (Problem 4.1) and the explicit Euler scheme (Problem 4.3) inherit the CS and CLS properties. Namely, under the condition (4.15), we have

$$|\Gamma^{m+1}| \leqslant |\Gamma^m| \quad (m = 0, 1, \ldots, \bar{m} - 1),$$

and, under the condition (4.16), we have

$$|\Gamma^{m+1}| = |\Gamma^m| + \mu_{\mathrm{CLS}}\tau_m \quad (m = 0, 1, \ldots, \bar{m} - 1).$$

A numerical simulation for the length-preserving polygonal curvature flow is shown in Figure 8.

5. Numerical computation

We describe an algorithm of our second order implicit scheme and show some numerical results. In this section, $\Gamma^m \in \mathcal{P}^*$ $(m = 0, 1, \ldots, \bar{m})$ denotes the numerical solution computed by the algorithm described in Section 5.1. All computations are performed in double precision.

5.1 *Algorithm*

We describe a numerical procedure for Problem 4.1. We suppose that an initial N-polygon $\Gamma^0 = \bigcup_{j=1}^{N} \overline{\Gamma_j^0}$ is given in a prescribed equivalence class $\mathcal{P}^*$, i.e., $\mathcal{P}^* = \mathcal{P}[\Gamma^0]$. In other words, the set $\{\boldsymbol{n}_j\}_{j=1}^N$ of normal vectors for $\mathcal{P}^*$ and the set $\boldsymbol{h}^0 = (h_1^0, \ldots, h_N^0) \in \mathbb{R}^N$ of heights of Γ_j^0 are given. The outer angles $\{\varphi_j\}_{j=1}^N$ and the quantities $\{a_j\}_{j=1}^N$, $\{b_j\}_{j=1}^N$ are computed from $\{\boldsymbol{n}_j\}_{j=1}^N$. We fix the maximum computation time T_* and the uniform time step $\tau = T_*/\bar{m}$ with the maximum time step $\bar{m}$.

Then $\Gamma^{m+1} \in \mathcal{P}^*$ is determined successively from $\Gamma^m \in \mathcal{P}^*$ at the mth discrete time $t_m = m\tau$ for $m = 0, 1, \ldots, \bar{m} - 1$ as follows. We suppose the set $\boldsymbol{h}^m = (h_1^m, \ldots, h_N^m) \in \mathbb{R}^N$ of heights of Γ_j^m are given. We can calculate the jth vertex $\boldsymbol{w}_j^m$ of Γ^m by (2.1) $(j = 1, \ldots, N)$. Our algorithm including the iteration scheme to obtain an approximation of Γ^{m+1} is as follows.

(1) Put $\bar{\boldsymbol{h}} := \boldsymbol{h}^m$.
(2) Define $\hat{\Gamma} \in \mathcal{P}^*$ with $\boldsymbol{h}(\hat{\Gamma}) = \bar{\boldsymbol{h}}$ and put $\hat{\boldsymbol{h}} := \bar{\boldsymbol{h}}$.
(3) Compute $\bar{\boldsymbol{h}} := \boldsymbol{h}^m + \boldsymbol{F}(\hat{\Gamma}, t_{m+1/2})\,\tau/2$.
(4) If $|\bar{\boldsymbol{h}} - \hat{\boldsymbol{h}}|_\infty \leqslant \varepsilon/2$, then go to step (6).
(5) Go to step (2).
(6) Put $\boldsymbol{h}^{m+1} := 2\bar{\boldsymbol{h}} - \boldsymbol{h}^m$.

We note that $\hat{\Gamma}$ and $\bar{\Gamma}$ (with $\boldsymbol{h}(\bar{\Gamma}) = \bar{\boldsymbol{h}}$) in step (3) correspond to $(\Lambda_m^{\nu}(\Gamma^m) + \Gamma^m)/2$ and $(\Lambda_m^{\nu+1}(\Gamma^m) + \Gamma^m)/2$, respectively. In the stopping condition (4), a small parameter $\varepsilon > 0$ is needed. In the following numerical computations, we chose $\varepsilon = 10^{-15}$.

5.2 *Numerical examples*

In the following examples, several numerical computations of the evolution of N-sided polygons will be shown. The numerical solutions were computed until the time T_* with the uniform time increment $\tau = T_*/\bar{m}$, where $\bar{m}$ is the maximum time step. The figures are depicted at every Mth time step. The problems except Example 7 have the CAS property with μ_{CAS}, and the numerical solution keeps this property with the error $\Delta = \max_{0\leqslant m<\bar{m}} |\mu_{\mathrm{CAS}} - \mu^m_{\mathrm{CAS}}|$, where $\mu^m_{\mathrm{CAS}} = (|\Omega^{m+1}| - |\Omega^m|)/\tau$ is the mth discrete area speed. The problem in Example 7 has the CLS property with μ_{CLS}, and the numerical solution keeps this property with the error $\Delta = \max_{0\leqslant m<\bar{m}} |\mu_{\mathrm{CLS}} - \mu^m_{\mathrm{CLS}}|$, where $\mu^m_{\mathrm{CLS}} = (|\Gamma^{m+1}| - |\Gamma^m|)/\tau$ is the mth discrete length speed. The following two tables indicate the data N, T_*, τ, M and Δ in each example.

TABLE 1
Numerical parameters and Δ for Examples 1 and 2.

	Ex.1: Figure 2			Ex.2: Figure 3	
	(a)	(b)	(c)	(a)	(b)
N	5	7	22	7	
T_*	0.2801	0.3136	0.335	1.55	1.55
τ	10^{-6}			10^{-4}	10^{-7}
M	2801	3136	3350	775	775000
Δ	5.04×10^{-10}	7.62×10^{-10}	1.56×10^{-9}	2.87×10^{-11}	2.96×10^{7}

TABLE 2
Numerical parameters and Δ for Examples 4–7.

	Ex.3: Figure 4		Ex.5: Figure 6	Ex.6: Figure 7		Ex.7: Figure 8
	(a)(b)(c)	(d)(e)(f)	(a)(b)(c)	(a)(b)(c)	(d)(e)(f)	(a)(b)(c)
N	9	12	12	32		18
T_*	7.56	19.4	20	10	3.65	0.27
τ	10^{-5}		10^{-4}	10^{-4}		10^{-4}
M	37800	97000	10000	5000	1825	27
Δ	1.51×10^{-9}	1.07×10^{-9}	2.81×10^{-7}	4.26×10^{-9}	1.42×10^{-10}	5.11×10^{-11}

5.2.1 *Example 1—polygonal curvature flow.* Figure 2 indicates the evolution of polygons solving Problem 3.2 for $N = 5$ in Figure 2(a), $N = 7$ in Figure 2(b), $N = 22$ in Figure 2(c), starting from the initial polygon being the outermost N-sided polygon which is a combination of an upper half of a regular $2(N-2)$-polygon and a triangle. Each solution polygon evolves from outside to inside and has the CAS property with $\mu_{\mathrm{CAS}} = -2\sum_{j=1}^{N} \tan(\varphi_j/2)$. The numerical solutions keep the CAS property very accurately as shown in Table 1.

5.2.2 *Example 2—backward polygonal curvature flow.* Problem 3.2 can be computed backward in time. Figure 3(a) indicates the evolution of solution polygons to the backward polygonal curvature flow $V_j(t) = \kappa_j(t)$ $(j = 1, \ldots, 7)$. The initial polygon is the innermost 7-sided polygon and the solution polygons evolve from inside to outside. The above process can be followed by our second order scheme accurately.

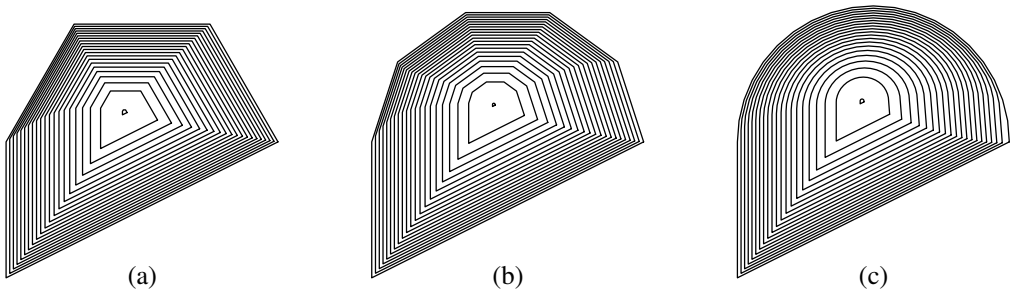

FIG. 2. Evolution by polygonal curvature flow: (a) $N = 5$, (b) $N = 7$, (c) $N = 22$.

We note that the backward curvature flow for smooth curves is ill-posed since it becomes a backward parabolic problem. Note that even for a 7-sided backward polygonal motion, it is difficult to obtain a numerical solution by means of the Euler scheme (Problem 4.6). Figure 3(b) indicates an easy breakdown of the Euler scheme despite using a smaller value of τ than for the second order scheme.

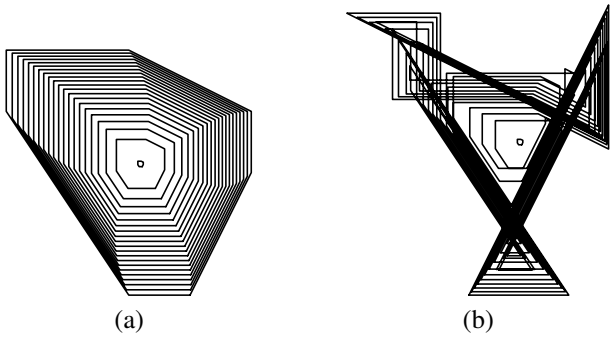

FIG. 3. Simulations of the backward polygonal curvature flow by the second order scheme (a) and by the Euler method (b).

5.2.3 *Example 3—area-preserving polygonal curvature flow.* Figure 4(b) (resp. (e)) shows two examples of polygonal motion according to Problem 3.3. The initial polygons are given in Figure 4(a) (resp. (d)). Figure 4(c) (resp. (f)) shows the initial polygon (dotted curve) and the final polygon. The solution has the CAS property with $\mu_{\text{CAS}} = 0$.

Both in Figures 4(a–c) and in Figures 4(d–f), there exist stationary solutions as shown in Figures 5 (b–c). The polygon starting from a symmetric initial shape approaches one of the stationary solutions and stays there for a while. However, since the stationary solution has a saddle-point instability, after a while, the polygon is drifted away from the stationary solution along the unstable manifold and loses its symmetry.

5.2.4 *Example 4—stationary solutions.* A polygon with constant polygonal curvature (i.e. $\kappa_1 = \cdots = \kappa_N$) is a stationary solution of Problem 3.3. Obviously, regular polygons are stationary solutions. Besides the regular polygons, we have infinitely many stationary solutions. For instance, an n-fold star-shaped polygon is a stationary solution, as also is the 6-fold star (Figure 5(a)). An

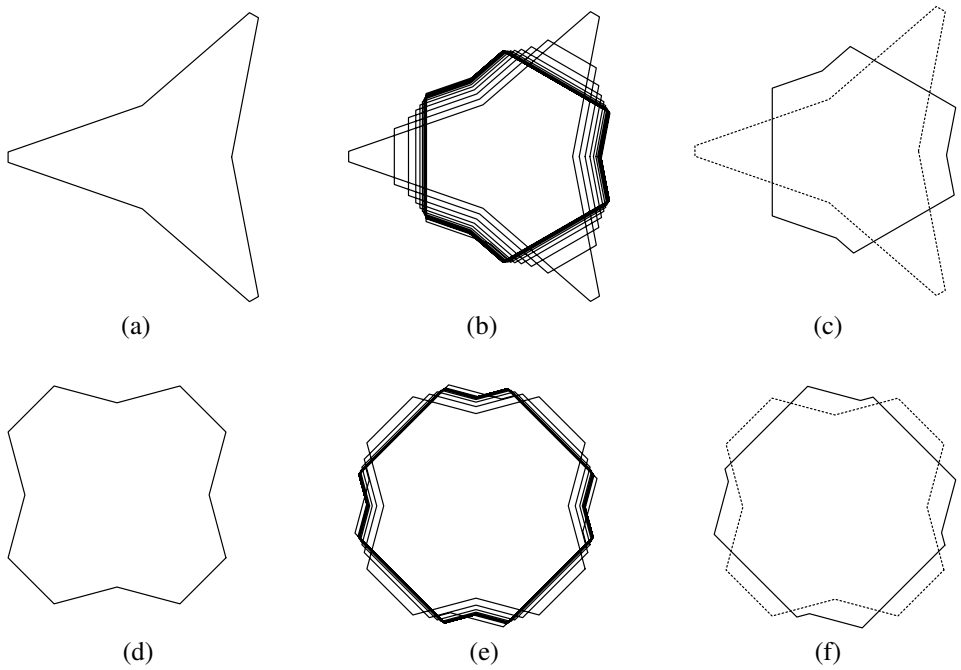

FIG. 4. Evolutions by the area-preserving polygonal curvature flow.

n-fold non-sharp star shaped polygon is a stationary solution, as also are the 3-fold (resp. 4-fold) non-sharp stars in Figure 5(b) (resp. (c)). For the n-fold non-sharp star polygon, there are two kinds of outer angles $\varphi_0 < 0$ and $\varphi_1 > 0$ and two kinds of edge lengths $d_1 < d_2$ with the corresponding polygonal curvatures $\kappa_1 = (\tan(\varphi_0/2) + \tan(\varphi_1/2))/d_1$ and $\kappa_2 = 2\tan(\varphi_1/2)/d_2$. We obtain a constant polygonal curvature polygon if $d_1/d_2 = (\tan(\varphi_0/2) + \tan(\varphi_1/2))/(2\tan(\varphi_1/2))$. The polygon in Figure 5(b) (resp. (c)) belongs to the same equivalence class of Figure 4(a–c) (resp. (d–f)).

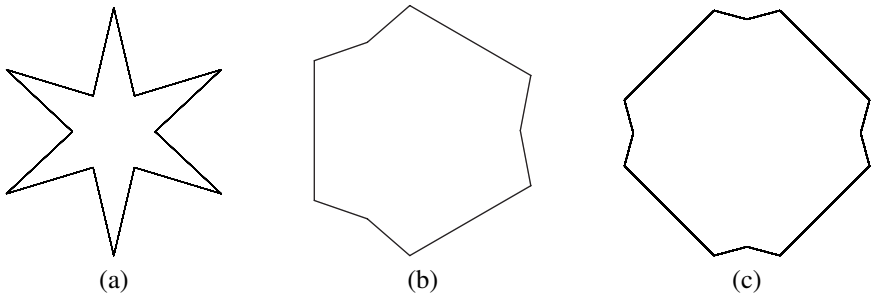

FIG. 5. Stationary solutions of Problem 3.3.

5.2.5 *Example 5—polygonal advected flow with constant area speed.* Figure 6(b) shows an example of polygonal motion according to Problem 3.4 with $\boldsymbol{u}(\boldsymbol{x}) = \boldsymbol{x}/(2\pi|\boldsymbol{x}|^2)$ which is a

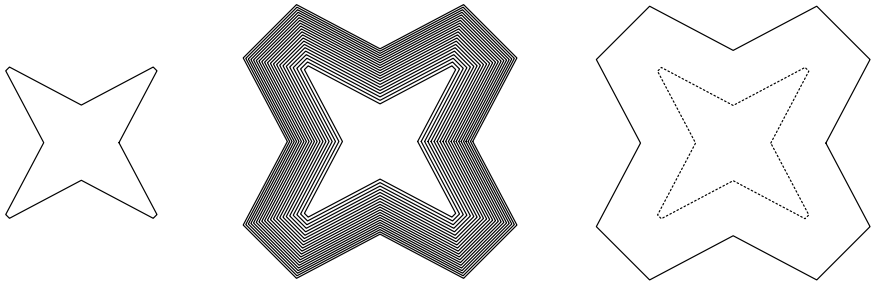

FIG. 6. Evolution by advected polygonal flow with constant area speed.

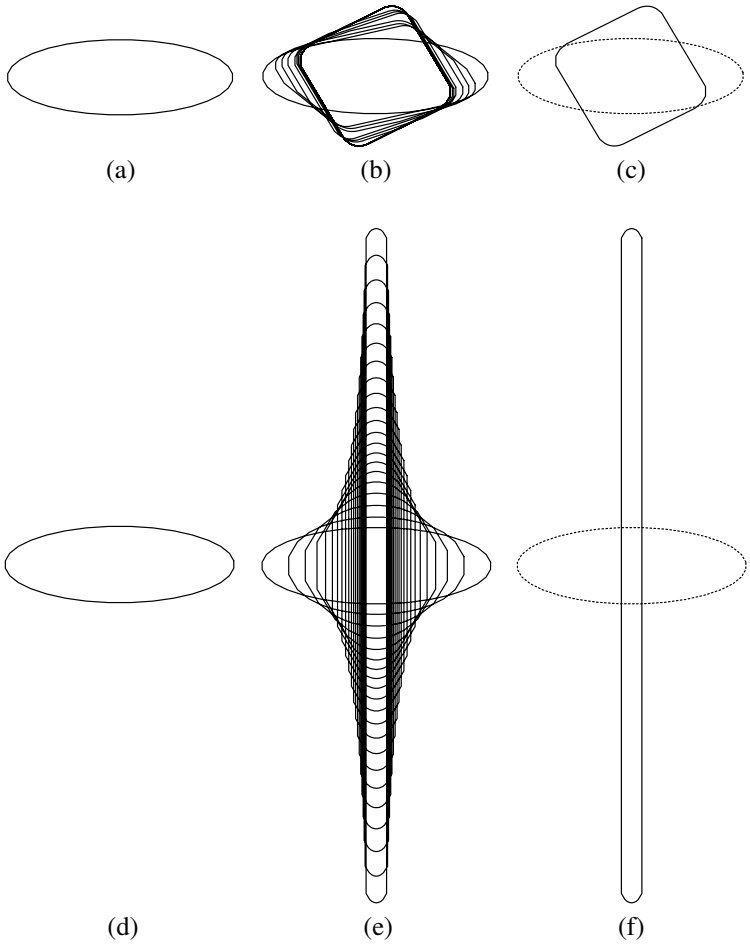

FIG. 7. Evolution by advected area-preserving polygonal curvature flow.

divergence-free vector field defined on $\mathbb{R}^2 \setminus \{\mathbf{0}\}$. The initial polygons are given in Figure 6(a), centered at the origin of coordinates.

Figure 6(c) shows the initial polygon (dotted curve) and the final polygon. The problem has the CAS property with $\mu_{\text{CAS}} = 1$. The numerical solution keeps the CAS property as accurately as shown in Table 2.

5.2.6 *Example 6—area-preserving polygonal advected-curvature flow.* Figures 7(b)(e) show two examples of polygonal motion combining Problems 3.3 and 3.4, i.e.,

$$V_j = \langle \kappa(\cdot, t) \rangle - \kappa_j(t) + \langle \boldsymbol{u} \rangle_j \cdot \boldsymbol{n}_j \quad (j = 1, \ldots, N).$$

The divergence-free vector field is given by $\boldsymbol{u}(\boldsymbol{x}) = x_1 x_2(-x_1, x_2)$ ((a)(b)(c)) and $\boldsymbol{u}(\boldsymbol{x}) = (-x_1, x_2)$ ((d)(e)(f)), respectively. The common initial polygon is given in Figure 7(a)(d), where the center is the origin of coordinates, and vertices are on the ellipse with ratio 3:1. Figure 7(c)(f) shows the initial polygon (dotted curve) and the final polygon. Both problems have the CAS property with $\mu_{\text{CAS}} = 0$ (area-preserving). The numerical solution preserves the areas as accurately as shown in Table 2.

5.2.7 *Example 7—length-preserving polygonal curvature flow.* Figure 8(b) shows the evolution of polygons according to the length-preserving polygonal curvature flow (4.17) given in Section 4.4. The initial polygon is the 18-sided polygon in Figure 8(a). Figure 8(c) indicates the initial polygon (dotted curve) and the final polygon. At the time close to T_*, the length of an edge (indicated by the arrow) tends to zero, and the computation stops. The length-preserving property ($\mu_{\text{CLS}} = 0$) is numerically realized with high accuracy as shown in Table 2.

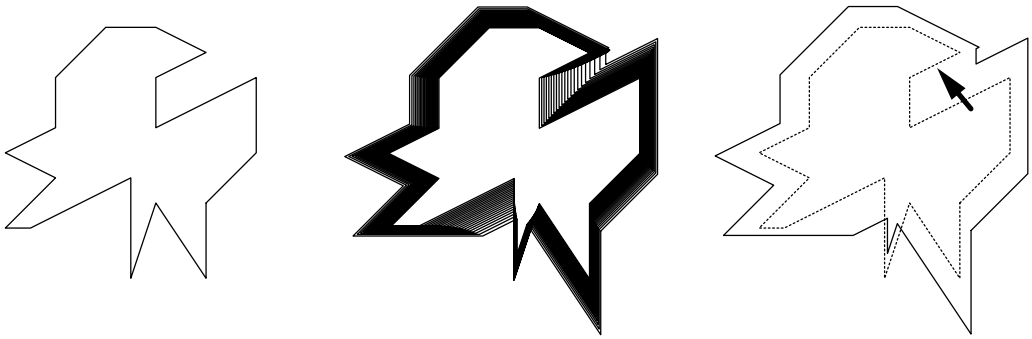

(a) (b) (c)

FIG. 8. Evolution by the length-preserving polygonal curvature flow.

Acknowledgements

The authors were partly supported by Czech Technical University in Prague, Faculty of Nuclear Sciences and Physical Engineering within the projects "Applied Mathematics in Physical and Technical Sciences" No. MSM6840770010, and the "Jindřich Nečas Center for Mathematical Modelling" No. LC06052 of the Czech Ministry of Education, Youth and Sports. The authors would like to thank the anonymous referee for her or his comments and suggestions.

REFERENCES

1. ANDREWS, B. Singularities in crystalline curvature flows. *Asian J. Math.* **6** (2002), 101–122. Zbl 1025.53038 MR 1902649
2. ANGENENT, S., & E. GURTIN, M. Multiphase thermomechanics with interfacial structure, 2. Evolution of an isothermal interface. *Arch. Ration. Mech. Anal.* **108** (1989), 323–391. Zbl 0723.73017 MR 1013461
3. GAGE, M. On an area-preserving evolution equation for plane curves. In: D. M. DeTurck (Ed.), *Nonlinear Problems in Geometry*, Contemp. Math. 51, Amer. Math. Soc. (1986), 51–62. Zbl 0608.53002 MR 0848933
4. GIGA, Y. *Surface Evolution Equations, A Level Set Approach*. Monographs Math. 99, Birkhäuser, Basel (2006). Zbl 1096.53039 MR 2238463
5. GIGA, M.-H., & GIGA, Y. Crystalline and level set flow—convergence of a crystalline algorithm for a general anisotropic curvature flow in the plane. In: *Free Boundary Problems: Theory and Applications, I* (Chiba, 1999), GAKUTO Int. Ser. Math. Sci. Appl. 13, Gakkōtosho, Tokyo (2000), 64–79. Zbl 0957.35122 MR 1793023
6. GIRÃO, P. M. Convergence of a crystalline algorithm for the motio of a simple closed convex curve by weighted curvature. *SIAM J. Numer. Anal.* **32** (1995), 886–899. Zbl 0830.65150 MR 1335660
7. GIRÃO, P. M., & KOHN, R. V. Convergence of a crystalline algorithm for the heat equation in one dimension and for the motion of a graph by weighted curvature. *Numer. Math.* **67** (1994), 41–70. Zbl 0791.65063 MR 1258974
8. ISHII, K., & SONER, H. M. Regularity and convergence of crystalline motion. *SIAM J. Math. Anal.* **30** (1999), 19–37. Zbl 0963.35082 MR 1646732
9. ISHIWATA, T., USHIJIMA, T. K., YAGISITA, H., & YAZAKI, S. Two examples of nonconvex self-similar solution curves for a crystalline curvature flow. *Proc. Japan Acad. Ser. A* **80** (2004), 151–154. Zbl 1077.53054 MR 2099341
10. ISHIWATA, T., & YAZAKI, S. On the blow-up rate for fast blow-up solutions arising in an anisotropic crystalline motion. *J. Comput. Appl. Math.* **159** (2003), 55–64. Zbl 1033.65055 MR 2022315
11. TAYLOR, J. E. Motion of curves by crystalline curvature, including triple junctions and boundary points. In: *Differential Geometry: Partial Differential Equations on Manifolds* (Los Angeles, CA, 1990), Proc. Sympos. Pure Math. 54, Amer. Math. Soc. (1993), Part I, 417–438. Zbl 0823.49028 MR 1216599
12. USHIJIMA, T. K., & YAZAKI, S. Convergence of a crystalline algorithm for the motion of a closed convex curve by a power of curvature $V = K^{\alpha}$. *SIAM J. Numer. Anal.* **37** (2000), 500–522. Zbl 0946.65071 MR 1740769
13. USHIJIMA, T. K., & YAZAKI, S. Convergence of a crystalline approximation for an area-preserving motion. *J. Comput. Appl. Math.* **166** (2004), 427–452. Zbl 1052.65082 MR 2041191
14. YAZAKI, S. Asymptotic behavior of solutions to an expanding motion by a negative power of crystalline curvature. *Adv. Math. Sci. Appl.* **12** (2002), 227–243. Zbl 1032.53059 MR 1909446
15. YAZAKI, S. On an area-preserving crystalline motion. *Calc. Var. Partial Differential Equations* **14** (2002), 85–105. Zbl 1143.37320 MR 1883601
16. YAZAKI, S. Motion of nonadmissible convex polygons by crystalline curvature. *Publ. Res. Inst. Math. Sci.* **43** (2007), 155–170. Zbl 1132.53036 MR 2317117
17. YAZAKI, S. Asymptotic behavior of solutions to an area-preserving motion by crystalline curvature. *Kybernetika* **43** (2007), 903–912. Zbl 1139.53032 MR 2388403